between $\Delta G^{\neq}_2$ and Gutmann donor number. If we assume that the dissociative mechanism is predominant in acetonitrile, the figure of Strasser *et al.* tells us that $\Delta G^{\neq}_2$ will be about 79 kJ/mol. This is 12-28 kJ/mol larger than observed $\Delta G^{\neq}$ value, which indicates that dissociative mechanism is improbable.

Acknowledgment. This research was supported financially in part by a grant (Project No. BSRI 93-309) from the Basic Science Research Institute Program, Ministry of Education, Korea, 1993.

References

1. Pedersen, C. D. *J. Am. Chem. Soc.* **1967**, *89*, 2495. *J. Am. Chem. Soc.* **1967**, *89*, 7017.
2. Lewison, F.; Ghirardelli, R. G.; Palcer, R. A. *Inorg. Chem.* **1989**, *28*, 3909.
3. Izatt, R. M.; Pawlak, K.; Bradshaw, J. S. *Chem. Rev.* **1991**, *91*, 1721.
4. Some examples are spectrophotometry (a, b), potentiometry (c), conductivity (d); (a) Drumhiller, J. A.; Montavon, F.; Lehn, J. M.; Taylor, R. W. *Inorg. Chem.* **1986**, *25*, 3751. (b) Sekhar, V. C.; Cheng, C. A. *Inorg. Chem.* **1986**, *25*, 2061. (c) Hay, R. W.; Puhari, M. P.; McLaren, F. *Inorg. Chem.* **1984**, *23*, 3033. (d) Cox, B. G.; Jedral, W.; Firman, P.; Schneider, H. *J. Chem. Soc., Faraday Trans.* **1981**, *2*, 486.
5. Weber, E.; Toner, J. L.; Goldberg, I.; Vogtle, F.; *et al.*, *Crown Ethers and Analogs*; John Wiley and Sons, 1989.
6. Seoung, W. M. Ph.D. Thesis, Seoul National University, 1993.
7. Reinhoudt, D. N.; Gray, R. T.; Smit, C. J.; Veenstraf, I. *Tetrahedron* **1976**, *32*, 1161.
8. Sandström, J. *Dynamic NMR Spectroscopy*; Academic Press, 1981.
9. Cox, B. G.; Garcia-Rosas, J.; Schneider, H. *J. Am. Chem. Soc.* **1981**, *103*, 1054.
10. some of them are about solvent effect (a, b, c), rigidity (d, e), anion effect (f); (a) Shchori, E.; Jagur-Grodzinski, J.; Shporer, M. *J. Am. Chem. Soc.* **1973**, *95*, 3842. (b) Strasser, B. O.; Popov, A. I. *J. Am. Chem. Soc.* **1985**, *107*, 7921. (c) Briere, K. M.; Detellier, C. *Can. J. Chem.* **1992**, *70*, 2536. (d) Szczygiel, P.; Shamsipur, M.; Hallenga, K.; Popov, A. I. *J. Phy. Chem.* **1987**, *91*, 1252. (e) Briere, K. M.; Detellier, C. *J. Phy. Chem.* **1992**, *96*, 2185. (f) Strasser, B. O.; Hallenga, K.; Popov, A. I. *J. Am. Chem. Soc.* **1985**, *107*, 789.
11. Shchori, E.; Jagur-Grodzinski, J.; Luz, Z.; Shporer, M. *J. Am. Chem. Soc.* **1971**, *93*, 7133.
12. Detellier, C. *Modern NMR Techniques and Their Application in Chemistry*; Marcel Dekker Inc., 1991, pp 521-566.
13. Greenberg, M. S.; Bodner, R. L.; Popov, A. I. *J. Chem. Phy.* **1973**, *77*, 2449.
14. Morris, D. F. C. *Struc. Bonding (Berlin)* **1968**, *4*, 63.
15. Pedersen, C. J. *J. Am. Chem. Soc.* **1970**, *92*, 386. The cavity size of 15C5 estimated is 170-220 pm and the cavity of X17C5 will be comparable to this.
16. Reinhoudt, D. N.; Gray, R. T.; De Jong, F.; Smit, C. J. *Tetrahedron* **1977**, *33*, 567.
17. Lin, J. D.; Popov, A. I. *J. Am. Chem. Soc.* **1981**, *103*, 3773.
18. Gutmann, V. *The Donor-Acceptor Approach to Molecular Interactions*; Plenum, New York, 1978.
19. Figure 4 of reference 10(b).

Topological Analysis on the Spinodal Decomposition and Interfacial Tension of Polymer-Solvent Systems

Jung Mo Son and Hyungsuk Pak*

Department of Chemistry, Seoul National University, Seoul 151-742, Korea
Received December 27, 1994

A topological theory has been introduced to extend the theory of Balsara and Nauman to evaluate the entropy of inhomogeneous polymer solutions. Previous theories have considered only the terms about the displacement of junction points, while the present theory has obtained a more complete expression for the entropy by adding the topological interaction terms between strands. There have been predicted the characteristics of the spinodal decomposition and the interfacial tension of polymer solutions from the resultant expression. It is exposed that the theoretically predictive values show good agreement with the experimental data for polymer solutions.

Introduction

Topological theories have recently played a great role in studying various physical properties including the elasticity of polymers. The theories which have systematically studied the rubber elasticity so far are the phantom network theories[1~6] headed by Flory *et al.* and the topological network theories[7~12] headed by Iwata *et al.* Since phantom network theories have dealt with the energies of rubber elasticity as only functions of the end-to-end distance between junction points, and have not considered the effect of interaction between chains by entanglement, these have recently retrogra-

ded. On the other hand, topological network theories have developed remarkably since these have explained very well the effect of interaction between chains by entanglement. Iwata has theoretically explained the various phenomena of rubber elasticity by applying topological theories to the polymer systems consisting of only a single kind of polymers.[10~12] The models with which he has dealt are mainly confined to the SCL (simple cubic lattice) ones,[11~12] and he did not obtain detailed transformation matrices and related topological contribution terms of entropy in conjunction with the tetrahedral lattice (THL) model (called the body-centered cubic lattice (BCL) model earlier by our previous work[13]). He has analyzed the theory of Balsara and Nauman about polymer solutions in view of topological approach. The question of how the entropy caused by strands is bound up with interaction between chains of polymer systems has systematically examined in detail. Here, a topological theory for polymer solutions has been evolved by assuming that the polymer solutions have the structure of the THL model. It is assumed that all the junction points of polymer solutions form the THL model for some average time interval.

In the present work, the entropy term caused by interaction between strands has been topologically derived based upon the THL model. We have topologically extended the theory of Balsara and Nauman by combining the obtained topological entropy term with the entropy one caused by displacement of junction points. In the result, a discrepancy between the original theory of Balsara and Nauman and experimental data is removed. The theoretically predictive values are in good agreements with the experimental data.

THL Model

This tetrahedral lattice (THL) model has been known as the body-centered cubic lattice (BCL) one by our previous work.[13] The distribution functions and transformation matrices about the THL model had already been offered by our previous work.[13~15] In the present work, the contribution term of entropy caused by interaction between polymer strands is derived from topological distribution functions by assuming that the structure of polymer-solvent systems forms a large aggregate of the THL model.

THL model is the one in which the junction points of polymer networks are located at the points of a body-centered cubic lattice, and in which the arrangement of four strands projected from each junction point always takes the tetrahedral structure. The picture of the three dimensional structure of the THL model is given in Figure 1, where solid lines denote linearly compressed strands and small circles represent junction points. Here a word strand means a polymer chain which joins two neighboring junction points. A word junction point means the jointing part of strands in the networks.

In the THL model, it is assumed that a polymer solute chain aggregate is regularly arranged at the lattice points, in turn with the solvent chain aggregate. For example, in Figure 1, the black closed circles including A and C represent the sets of junction points of polymer solute molecules, and the white open circles including B and D represent those of polymer solvent molecules. Especially, in the case that solvent molecules have lower molecular weight which does not form cross-link, the open circles represent the sites to which the end point of solvent molecules attach. In short, the network structure of the THL model is composed of the aggregate of polymer solute molecules and the aggregate of solvent molecules. In each chain aggregate, junction points are classified into two categories according to the methods of their combination with neighboring strands. One is the set of junction points corresponding to the apexes of lattices (*i.e.*, the junction point surrounded with a regular square of Figure 1), and the other to the body centers of lattices (*i.e.*, the junction point surrounded with a regular triangle of Figure 1).

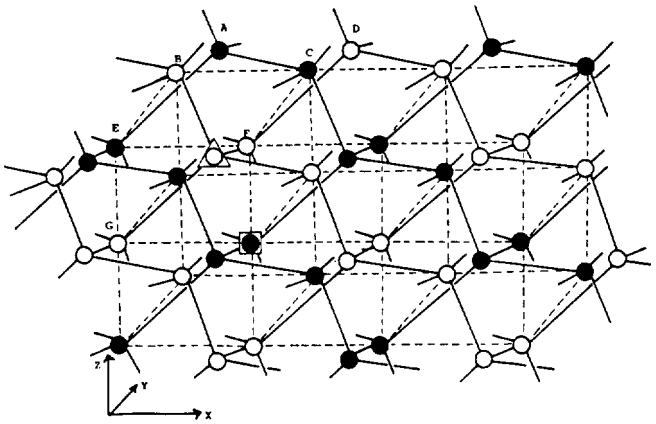

Figure 1. The three dimensional structure of the THL (tetrahedral lattice) model, where solid lines denote strands and small circles represent junction points. The black closed circles including A and C represent the sets of junction points of polymer solute molecules, and white open circles B and D represent those of polymer solvent molecules. A junction point, J_{ev}, is plotted as the junction point surrounded with a regular square. A junction point, J_{od}, is plotted as that with a regular triangle. The length of $\overline{BE}$, $\overline{EF}$, and $\overline{EG}$ is all two without unit.

Let J_{ev}'s be junction points of the former and J_{od}'s the latter. For either J_{ev}'s or J_{od}'s, two different spatial orientations per junction point can be allocated in the way of combination with four neighboring strands around a given junction point. The effects of these two arrangements, however, are essentially identical in view of contribution to the free energy of the system, so it doesn't matter which of them is chosen in going on discussing. In usual, it is convenient to select a J_{ev} in the central part of the system as an origin of the coordinates.

Conveniently, if the length of an edge of lattices is taken as two without unit (*i.e.*, the distance of $\overline{BE}$, $\overline{EF}$, and $\overline{EG}$ is all two in Figure 1), the coordinates of every junction point can be readily described as the set of three components having only values of integers. Figure 2 represents the characteristic combination modes of strands around the general junction points J_{ev}'s and J_{od}'s, and shows the spatial orientations of strands defined on the basis of a J_{ev}, in addition to the coordinates of junction points.

Independently of J_{ev} or J_{od}, if l is taken as a position vector, the following equations give its components and their areas;

$$l=(i,\ j,\ k)$$

$$i=-I,\ -I+1,\ \cdots,\ I-1,\ I$$

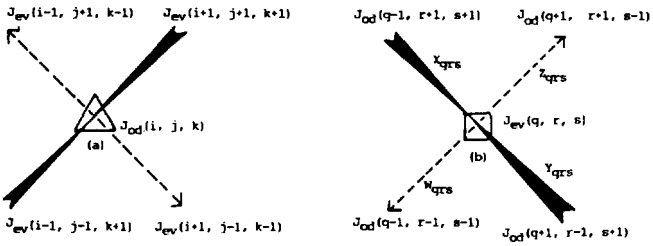

Figure 2. The characteristic combination modes of strands around the general junction points J_{od} (a) J_{ev} (b). This picture shows the spatial orientations of strands defined on the basis of a J_{ev}, in addition to the coordinates of junction points.

$$j=-J,\ -J+1,\ \cdots,\ J-1,\ J$$
$$k=-K,\ -K+1,\ \cdots,\ K-1,\ K \qquad (1)$$

where I, J, and K all take the values of positive integers. It is necessary to note that the components of every J_{ev} all have values of even integers, and that those of every J_{od} have only values of odd integers. The spatial orientations of all the strands in the system are deduced to only four, as plotted in Figure 2(b). Conveniently, let σ_l or $\sigma_{i,j,k}$ ($\sigma=X$, Y, Z, and W) be a symbol which represents a strand. Then the four spatial orientations of strands in the system are defined as

$$X_{i,j,k}=\text{strand from } J_{ev}(i,\ j,\ k) \text{ to } J_{od}(i-1,\ j+1,\ k+1)$$
$$Y_{i,j,k}=\text{strand from } J_{ev}(i,\ j,\ k) \text{ to } J_{od}(i+1,\ j-1,\ k+1)$$
$$Z_{i,j,k}=\text{strand from } J_{ev}(i,\ j,\ k) \text{ to } J_{od}(i+1,\ j+1,\ k-1)$$
$$W_{i,j,k}=\text{strand from } J_{ev}(i,\ j,\ k) \text{ to } J_{od}(i-1,\ j-1,\ k-1) \qquad (2)$$

The picture for these orientations is given in Figure 2(b).

The entropy term caused by interaction between strands, ΔS_{top}, can be derived by using the contact distribution functions of the THL model. The entropy change is called as the topological entropy change of polymer chains. For the THL model, the single contact probability between two strands, $g_p(r_i)$, and the double one between two strands, $h_p(r_i)$, are given by[13~15]

$$g_p(r_i)=m^{-2}\sum_{\mu=1}^{m^2} P_{ph}(O_\mu|r_i)$$
$$h_p(r_i)=m^{-2}[g_p(r_i)]^{-1}\sum_{\mu=1}^{m^2}\sum_{\mu'=1}^{m^2} P_{ph}(O_{\mu,\mu'}|r_i) \qquad (3)$$

where m is the number of submolecules in a strand, and r_i is the position vector of the ith strand from the reference junction point. $P_{ph}(O_\mu|r_i)$ is the single contact distribution function between chains, and $P_{ph}(O_{\mu,\mu'}|r_i)$ is the double one of the phantom network. $P_{ph}(O_\mu|r_i)$ and $P_{ph}(O_{\mu,\mu'}|r_i)$ are represented as

$$P_{ph}(O_\mu|r_i)=(3m^2/2\pi l_i^2\bar{u}_i\bar{u}_i\bar{v}_i\bar{v}_iK_1)^{3/2}\exp\left(\frac{-3(K_3-K_{2i}^2/K_{1i})}{2l_i^2}\right) \qquad (4)$$

and

$$P_{ph}(O_{\mu,\mu'}|r_i)=(9m^2/4\pi l_i^4\bar{u}_i\bar{v}_iu_i'v_i'\Delta u_i\Delta v_i\|K_1\|)^{3/2}$$
$$\exp\left(\frac{-3(K_3-K_2K_1^{-1}K_{2i})}{2l_i^2}\right) \qquad (5)$$

where l_i^2 is the root mean squared end-to-end distance of the ith strand, and where u_i and u_i' stand for positions of an a segment of i strand and v_i and v_i' stand for positions of a b segment of the same strand. $\bar{u}_i$, $\bar{v}_i$, Δu_i, and Δv_i have the relation that $\bar{u}_i=m-u_i$, $\bar{v}_i=m-v_i$, $\Delta u_i=|u_i-u_i'|$, and $\Delta v_i=|v_i-v_i'|$, respectively. K_{1i}, K_{2i}, and K_3 of Eqs. (4) and (5) are given by

$$K_1=\begin{pmatrix} 1/\bar{u}_i+1/\bar{v}_i+1/\Delta u_i+1/\Delta v_i & -1/\Delta u_i-/\Delta v_i \\ -1/\Delta u_i-1/\Delta v_i & 1/u_i'+1/v_i'+1/\Delta u_i+1/\Delta v_i \end{pmatrix}$$
$$K_2=\begin{pmatrix} r_a'/\bar{u}_i+r_b/v_i' \\ r_a/u_i'+r_b'/\bar{v} \end{pmatrix} \qquad (6)$$
$$K_3=r_a'^2/\bar{u}_i+r_a^2/u_i'+r_b'^2/\bar{v}_i+r_b^2/v_i'-(r_a-r_a')^2/m+(r_b-r_b')^2/m$$

The $\|K_1\|$ of Eq. (5) is a determinant of K_1.

The number of distinguishable arrangements caused by single contact among all the strands, Ω_g, is given by

$$\Omega_g=(1/n_1!)\prod_{i=1}^{n_1-1} g_p(r_i)$$
$$=(1/n_1!)\prod_{i=1}^{n_1-1}\left(g_p(r_i)m^{-2}\sum_{\mu=1}^{m^2} P_{ph}(O_\mu|r_i)\right) \qquad (7)$$

n_1 being the number of lattice sites available to the $(i+1)$th strand.

The number of distinguishable arrangement caused by double contact among all the strands, Ω_h, is represented by

$$\Omega_h=(1/n_1!)\prod_{i=1}^{n_1-1} h_p(r_i)$$
$$=(1/n_1!)\prod_{i=1}^{n_1-1}\left((g_p(r_i)m^{-2})^{-1}\sum_{\mu=1}^{m^2}\sum_{\mu'=1}^{m^2} P_{ph}(O_{\mu,\mu'}|r_i)\right) \qquad (8)$$

Evolving Eqs. (7) and (8) by following the procedure offered in Refs. 10-15, the equations for Ω_g and Ω_h are obtained as follows;

$$\Omega_g=\Omega_{FH}\in m\ \ln((1-\phi)^{1/4}/(1-\phi-0.5\phi^2)^{3/4}) \qquad (9)$$

and

$$\Omega_h=\Omega_{FH}\in m\ \ln((1-\phi)^{1/4}/(1-\phi-0.5\phi^2)^{1/2}) \qquad (10)$$

where $\phi(r)$ is the local polymer volume fraction at r from the reference point. The number of distinguishable arrangements of the Flory-Huggins's theory,[16] Ω_{FH}, and the variable $\in$ are given by

$$\Omega_{FH}=(1/n_1!)(\{z(z-1)^{m-2}\}/n_o^{m-1})^{n_1} \qquad (11)$$
$$\in=(1/4)\ (\nabla^2\phi),\ a^2\ n_o \qquad (12)$$

where z is the coordination number of the lattice, n_o is the number of the lattice sites, and a is the length of a strand. The number 4 in the denominator of Eq. (12) represents four directions of the strands attached to junction points. Thus the total number of topologically distinguishable arrangements caused by interaction among all the strands, Ω_{top}, is given by

$$\Omega_{top}=\Omega_g+\Omega_h$$
$$=\Omega_{FH}\in m\ \ln((1-\phi)^{1/2}/(1-\phi-0.5\phi^2)^{5/4}) \qquad (13)$$

Eq. (13) is one of the most important parts of our present

work, and a very valuable expression obtained by expanding the topological theory of Iwata to the THL model.

For phantom network theories, the entropy of polymer systems has been analyzed so far only by the contribution terms caused by displacement of junction points. In topological network theories, the change of entropy and free energy has been more completely considered by adding the contribution terms of entropy caused by interaction among strands to those caused by displacement of junction points.

Eq. (13) has important meanings in the fact that it offers the source of topological entropy based upon the structure of the polymer network of the THL model. In the next section, we consider how Eq. (13) contributes to expanding the theory of Balsara and Nauman, how it removes the discrepancy between theoretically predictive values and experimental data which the theory of Balsara and Nauman did not solve, and how it explains good agreement between theoretical values and experimental data.

Topological Analysis of the Balsara and Nauman's Theory

This section is composed of deriving the mixed entropy of polymer-solvent systems by combining the phantom network entropy of junction points with the topological entropy term of strands obtained in the previous section after obtaining the entropy caused by displacement of junction points, called the phantom network entropy. In the first place, the process of deriving of the phantom network entropy by Balsara and Nauman is described from now on.[17]

Consider the polymer network of the THL model as an aggregate of n lattice sites which contains a certain number of polymer molecules. It is assumed that these molecules are uniformly distributed throughout the n sites, except for a small region centered around a lattice site. Now such a small region is our system of interest. Let n_o be the number of sites contained in such a small region. It is necessary to estimate the effect of the nonuniformity of the polymer concentration on the entropic contribution of the lattice site at o.

It is assumed that the concentration gradients are small and the system is large compared with molecular dimensions. Namely, the system contains a large number of molecules. It is important to evaluate the number of ways of adding the $(i+1)$th polymer molecule to the lattice consisting of n_o sites, including the i polymer molecules added previously. Molecules should be arranged in a way that establishes and preserves the concentration gradient. In other words, the number of available sites is not equal to the number of vacant sites. Actually, larger proportions of vacant sites are available at the points where the existent concentration is high because it must remain high after the new molecules are placed.

As offered previously, let m be the number of submolecules contained in a strand. The number of options available to the first segment of the $(i+1)$th polymer chain is given by $(n\ (n_o-im)$. The number of ways of arranging the $(i+1)$th molecule, ν_{i+1} is given by

$$\nu_{i+1}=(n_o-im)\ \underbrace{X}_{\text{1st segme}}\ \underbrace{z(f_{1i})}_{\text{n2nd}}\ X\ \underbrace{(z-1)(f_{2i})}_{\text{3rd}}\ X\cdots X\ \underbrace{(z-1)(f_{mi})}_{m\text{th segment}} \tag{14}$$

where f_{ni} is the fraction of sites available to the nth segment of the $(i+1)$th strand and z is the coordination number of the lattice. The local polymer volume fraction at r from the reference, $\phi(r)$, is assumed to be expressed as a Taylor series in terms of the volume fraction at o.[18]

$$\phi(r)=\phi_o+[r\cdot\nabla)\Phi]_o+(1/2)[(r\cdot\nabla)^2\Phi]_o \tag{15}$$

For the THL model, the average volume fraction at a distance L from a randomly chosen lattice site can be expressed as

$$\bar{\Phi}(\bar{L})=\Phi_{AV}+(1/4)(\nabla^2\Phi)_o\ L^2 \tag{16}$$

where Φ_{AV} is the volume fraction averaged over the n_o sites. When a fixed concentration gradient is maintained, the fraction of vacant sites which are available to a given molecular segment decreases as the concentration increases and increases as the concentration decreases. For the THL model, the fractional availability is given by

$$f_{ni}=[1-im/n_o-(1/4)(\nabla^2\Phi)_o na^2] \tag{17}$$

where it is assumed that polymer strands are ideal chains so that the average extension of n segments may be na^2, a being the length of each segment. Therefore,

$$\nu_{i+1}=(n_o-im)z[1-im/n_o-(1/4)(\nabla^2\Phi)_o a^2](z-1)[1-im/n_o-(1/4)\cdot(\nabla^2\Phi)_o 2a^2]\cdots(z-1)[1-im/n_o-(1/4)(\nabla^2\Phi)_o ma^2] \tag{18}$$

or

$$\nu_{i+1}=[(n_o-im)/(n_o^{m-1})]z(n_o-im+\in)(z-1)(n_o-im+2\in)\cdots(z-1)(n_o-im+m\in) \tag{19}$$

where $\in$ is given by Eq. (12). Operating Eq. (19) so that only terms of order $\in$ may be retained, consistent with the assumption of small concentration gradients, we obtain

$$\nu_{i+1}=[(n_o-im)^m(z-1)^{m-2}/n_o^{m-1}][1+\{\in/(n_o-im)\}\{m(m+1)/2\}] \tag{20}$$

The total number of distinguishable arrangements, Ω_{ph}, is represented as

$$\Omega_{ph}=(1/n_1!)\prod_{i=0}^{n_1-1}\nu_{i+1} \tag{21}$$

Substitution of Eq. (20) into Eq. (21) on the condition that the terms of order $\in$ are retained gives

$$\Omega_{ph}=\frac{1}{n_1!}\left(\frac{z(z-1)^{m-2}}{n_o^{m-1}}\right)^{n_1}\left(1+\frac{\in\ m(m+1)}{2}\left[\frac{1}{n_o}+\frac{1}{n_o-m}+\cdots+\frac{1}{n_o-(n_1-1)m}\right]\right) \tag{22}$$

As known generally,

$$\sum_{k=1}^{n}\frac{1}{k}=0.577215+\ln\ n+\frac{1}{2n}-\cdots \tag{23}$$

For large n_o and n_1, Ω_{ph} can be accurately expressed as

$$\Omega_{ph}=\frac{1}{n_1!}\left(\frac{(z(z-1)^{m-2}}{n_o^{m-1}}\right)^{n_1}\left(1+\frac{\in\ m(m+1)}{2}\ \ln\left[\frac{n_o}{n_o-n_1m}\right]\right) \tag{24}$$

In the case that $m \gg 1$, Eq. (24) is transformed into

$$\Omega_{ph}=\Omega_{FH}(1+(\in M/2)\ln[1-\bar{\phi}]^{-1}) \tag{25}$$

where $\bar{\phi}$ is the averaged polymer concentration in the n_o sites, and Ω_{FH} is given in Eq. (11).

Balsara and Nauman offered Eq. (25) as the core of their theory, and regarded Eq. (25) as the equation from which the entropy of polymer-solvent systems could be obtained. As mentioned previously, however, Eq. (25) is only the partition function (the number of distinguishable arrangements) of a phantom network theory obtained by the contribution due to displacement of junction points. Therefore, the topological partition, Eq. (13), must be added to Eq. (25) in order to obtain the entropy of polymer-solvent systems more completely. Shortly speaking, the total partition function of the mixed systems, Ω, is obtained by adding Eq. (13) to Eq. (25). Namely,

$$\begin{aligned}\Omega&=\Omega_{ph}+\Omega_{top}\\&=\Omega_{FH}(1+(\in m/2)\ \ln[1-\bar{\phi}]^{-1})+\Omega_{FH}\ \in m\ \ln((1-\bar{\phi})^{1/2}/(1-\bar{\phi}-0.5\bar{\phi}^2)^{5/4})\\&=\Omega_{FH}(1+(\in m/2)\ \ln[1-\bar{\phi}]^{-1})+\Omega_{FH}\ \in m((\ln[1-\bar{\phi}])/2-(5/4)\ \ln(1-\bar{\phi}-0.5\ \bar{\phi}^2))\\&=\Omega_{FH}(1+(\in m/2)\ \ln[1-\bar{\phi}]^{-1})+\Omega_{FH}\ \in m(-(\ln[1-\bar{\phi}])/2+(5/4)\ \ln[1-\bar{\phi}-0.5\ \bar{\phi}^2]^{-1})\\&=\Omega_{FH}(1+(5\in m/4)\ \ln[1-\bar{\phi}-\bar{\phi}^2]^{-1})\end{aligned} \tag{26}$$

Ω of Eq. (26) is a position function indispensable to obtaining the entropy of a mixed system. Eq. (26) has important meanings in the fact that it is a more complete expression of describing the entropy change of a mixed system, and an equation of combing a topological network theory with a phantom network theory. Similarly to the case of Eq. (13), thus Eq. (26) is also one of important parts obtained in our present work.

Letting Ω_p and Ω_s be the number of distinguishable arrangements of the polymer and solvent molecules before mixing, the total entropy change on mixing, ΔS, is given by

$$\Delta S=k(\ln\ [\Omega_{FH}/\Omega_p\Omega_s]+\ln\ [1+(5\in m/4)\ \ln\{1-\bar{\phi}-0.5\bar{\phi}^2\}]) \tag{27}$$

where k is the Boltzmann constant.

Now consider the entropic contribution due to the lattice site located at 0, ΔS_s. Assuming slow spatial variations in ϕ, this can be evaluated by dividing Eq. (27) by n_o and replacing $\bar{\phi}$ by the local volume fraction ϕ.

$$\Delta S_s=\frac{k}{n_o}(\ln\ [\Omega_{FH}/\Omega_p\Omega_s]+\ln\ [1-(5n_oma^2\nabla^2\phi/24)\ \ln\{1-\bar{\phi}-0.5\bar{\phi}^2\}]) \tag{28}$$

It is necessary to note that both $\nabla^2\phi$ and ϕ are now evaluated at the reference point o. Neglecting terms involving $\in^2$, then

$$\Delta S_s=\Delta S_{FH}-\frac{5kma^2}{24}\ \ln(1-\phi-0.5\phi^2)\nabla^2\phi \tag{29}$$

where ΔS_{FH} is the Flory-Huggins's entropy of mixing per lattice site. Integrating Eq. (29) over the volume of the system, V, the mixed entropy of an inhomogeneous system, ΔS_m, is given by[18]

$$\Delta S_m=\int_v[s(\phi)-5kma^2\rho/24(1-\phi-0.5\phi^2)]dv \tag{30}$$

where ρ is the number of sites per unit volume, and $s(\phi)$ is the mixed entropy per unit volume of the perfectly homogeneous mixture. An expression for the free energy of mixing of the system, ΔG, can be obtained by combining the mixed enthalpy of an inhomogeneous polymer solution with Eq. (30). Expressing ΔG in the Landau-Ginzburg's form,[17] then

$$\Delta G=\int_v[g(\phi)+\kappa(\nabla\phi)^2]dv \tag{31}$$

where $g(\phi)$ is the Flory-Huggins's free energy of mixing per unit volume, and for the THL model k is represented by

$$\kappa=\frac{RT}{\bar{v}_s}\ \frac{R_G^2}{6}\ [\chi+5/(2-2\phi-\phi^2)] \tag{32}$$

where χ is the Flory-Huggins's interaction parameter, $\bar{v}_s$ is the molar volume of the solvent, and R_G is the radius of gyration of the ideal polymer chain. Generally, κ can be regarded as the penalty related with the occurrence of gradients in a given solution. Eq. (32) predicts that this penalty increases as the concentration of polymers increases, and actually the penalty approaches infinity near the bulk state ($\phi \rightarrow 1$).

Spinodal Decomposition of Polymer-Solvent Systems

The characteristics of the spinodal decomposition of polymer-solvent systems can be predicted by Eqs. (31) and (32). The analysis discussed here is based on the linearized theory of spinodal decomposition by Cahn.[9] According to the Cahn's theory, the wavelength of concentration fluctuation, λ_m, is given by

$$\lambda_m=4\pi[-\kappa/g''(\phi)]^{1/2} \tag{33}$$

The λ_m of Eq. (33) plays a role of dominating the initial stages of the decomposition of an unstable solution. $g''(\phi)$ can be evaluated by the Flory-Huggins's theory as follows;

$$g''(\phi)=\frac{2RT}{\bar{v}_s}(\chi_{T_s}-\chi_T) \tag{34}$$

where T is the temperature of unstable solution, T_s the spinodal temperature of the solution, and χ_T and χ_{T_s} are the value of χ at T and T_s, respectively. Combining of Eqs. (32)-(34) gives

$$\lambda_m=(2\pi R_G/3^{1/2})[(\chi_T-\chi_{T_s})/\{\chi_T+5/(2-2\phi-\phi^2)\}]^{-1/2} \tag{35}$$

Assuming that

$$\chi_{T_s}/\chi_T=T/T_s \tag{36}$$

then

$$\lambda_m=(2\pi R_G/3^{1/2})[(T_s/T-1)/\{T_s/T+5/(\chi_{T_s}(2-2\phi-\phi^2)\}]^{-1/2} \tag{37}$$

Referentially writing down λ_m of the Balsara and Nauman's

theory, then

$$\lambda_m=(2\pi R_G/3^{1/2})[(T_s/T-1)/[T_s/T+3/|\chi_{T_s}(1-\phi)|]^{-1/2} \quad (37')$$

Neglecting the entropic contribution of junction points and strands in Eq. (37), the Van Aarsten's equation for λ_m is given as follows:

$$\lambda_m=(2\pi R_G/3^{1/2})[1-T_s/T]^{-1/2} \quad (38)$$

Interfacial Tension of Demixed Polymer Solutions

Cahn and Hilliard had already discovered the relationship between interfacial tension and free energy of inhomogeneous solutions.[18] According to their theory, the interfacial tension, σ, between two binary liquid phases α and β at equilibrium is given by

$$\sigma=2\int_{\phi^\alpha}^{\phi^\beta}[\kappa\ \Delta g(\phi)]^{1/2}\ d\phi \quad (39)$$

where $\Delta g(\phi)$ is the homogeneous free energy per unit volume of a mixture with concentration, ϕ, referred to a standard state of an equilibrium mixture of α and β (see Ref. 18 for details). Letting α and β be the dilute phase and the concentration phases, respectively, $\Delta g(\phi)$ about a polymer-solvent system obeying the Flory-Huggins is represented as follows;

$$\Delta g=\frac{RT}{v_s}\left(\frac{\phi}{m}(\mu_p-\mu_p^\circ)+(1-\phi)(\mu_s-\mu_s^\circ)\right) \quad (40)$$

where μ_p and μ_s are scaled chemical potentials of the polymer and solvent, respectively. μ_p and μ_s are given by

$$\mu_p=\ln\ \phi-(m-1)(1-\phi)+m\chi(1-\phi)^2 \quad (41)$$

$$\mu_s=\ln\ (1-\phi)+(1-1/m)\phi+\chi\ \phi^2 \quad (42)$$

The values of μ_p and μ_s evaluated at equilibrium, μ_p° and μ_s°, are given by

$$\mu_p^\circ=\mu_p(\phi^\alpha)=\mu_p(\phi^\beta)$$
$$\mu_s^\circ=\mu_s(\phi^\alpha)=\mu_s(\phi^\beta) \quad (43)$$

Combing Eq. (32) with Eq. (39) gives

$$\sigma=\frac{2R\ T\ R_G}{6^{1/2}v_s}\int_{\phi^\alpha}^{\phi^\beta}\left(\left[\chi+\frac{5}{2-2\phi-\phi^2}\right]\left[\frac{\phi}{m}(\mu_p-\mu_p^\circ)+(1-\phi)\ (\mu_s-\mu_s^\circ)\right]\right)^{1/2}d\phi \quad (44)$$

Referentially describing the interfacial tension, σ, of the Balsara and Nauman's theory in order to compare Eq. (44) with their equation, then

$$\sigma=\frac{2R\ T\ R_G}{6^{1/2}v_s}\int_{\phi^\alpha}^{\phi^\beta}\left(\left[\chi+\frac{3}{1-\phi}\right]\left[\frac{\phi}{m}(\mu_p-\mu_p^\circ)+(1-\phi)\ (\mu_s-\mu_s^\circ)\right]\right)^{1/2}d\phi \quad (44')$$

Results and Discussion

The results of the Balsara and Nauman's theory for polymer-solvent systems are expanded by adding those of a topological network theory of dealing with the interaction between strands in order to remove the discrepancy between the original theory of Balsara and Nauman and experimental data nearly to the zero it.

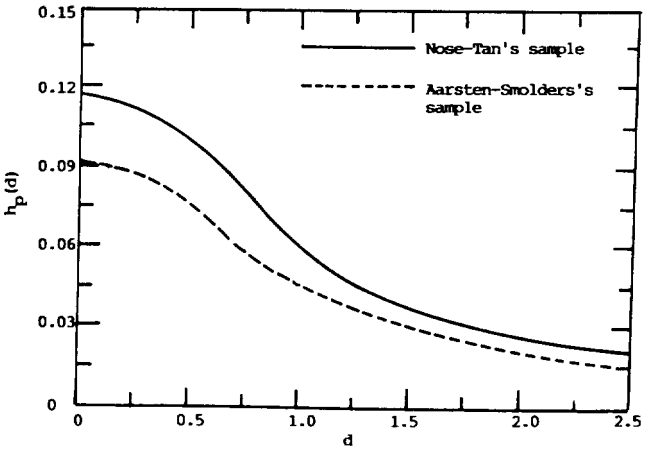

Figure 3. The $h_p(d)$ as functions of d, which is a distance between the centers of the strands, for the THL model. The solid line represents the curves obtained by the Nose-Tan's sample when the root mean squared end-to-end distance of a strand, q, is 0.32 $m^{1/2}a$, and the dashed one represents that by the Aarsten-Smolders's when q is 0.47 $m^{1/2}a$.

It is assumed that the polymer-solvent systems considered here are composed of the polymer networks of the THL model. The detailed structure for these polymer networks is plotted in Figure 1. The polymer network of joining the junction points represented by black closed circles is an aggregate of polymer solute, that by white open circles is one of solvents. It is regarded that the THL model offered here is the reasonable structure of polymer networks when attractive and repulsive force between chains are all considered. In polymer networks of the THL structure, the way of arranging of strands around junction points is plotted in Figure 2. The core of topological network theories is in the fact that the interaction between strands is regarded as the principal contribution term to entropy and free energy for polymer-solvent systems. Interaction between strands is classified into the term caused by single contact and that by double. A central distance between strands is given by

$$d=\frac{|r_a+r_a'-r_b-r_b'|}{2\ m^{1/2}\ a} \quad (45)$$

where r_a and r_a' are the position vectors representing both end points of the a strand, and $_b$ and r_b' those of the b strand. $g_p(r)$ and $h_p(r)$ of Eq. (3) are readily transformed into $g_p(d)$ and $h_p(d)$, respectively. In Figure 3, there are shown the calculated curves of $h_p(d)$ about the Aarsten-Smolders's sample[22] and the Nose-Tan's sample[22] for the THL model structure. In Figure 4, there are shown the calculated curves of $g_p(d)$ about the Aarsten-Smolders's sample and Nose-Tan's sample for the THL model structure. In Figures 3 and 4, the solid lines represent the curves obtained by the Nose-Tan's sample when the root mean squared end-to-end distance of a strand, q, is 0.32 $m^{1/2}a$, and the dashed lines represent that by the Aarsten-Smolders's when q is 0.47 $m^{1/2}a$. Since the value of q of each sample strand is peculiarly determined by various factors such as degree of polymerization,

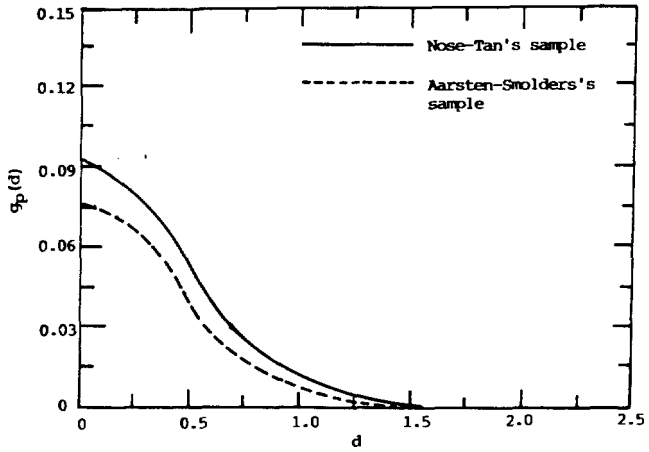

Figure 4. The $g_p(d)$ as functions of d, which is a distance between the centers of the strands, for the THL model. The solid line represents the curves obtained by the Nose-Tan's sample when the root mean squared end-to-end distance of a strand, q, is 0.32 $m^{1/2}a$, and the dashed one represents that by the Aarsten-Smolders's when q is 0.47 $m^{1/2}a$.

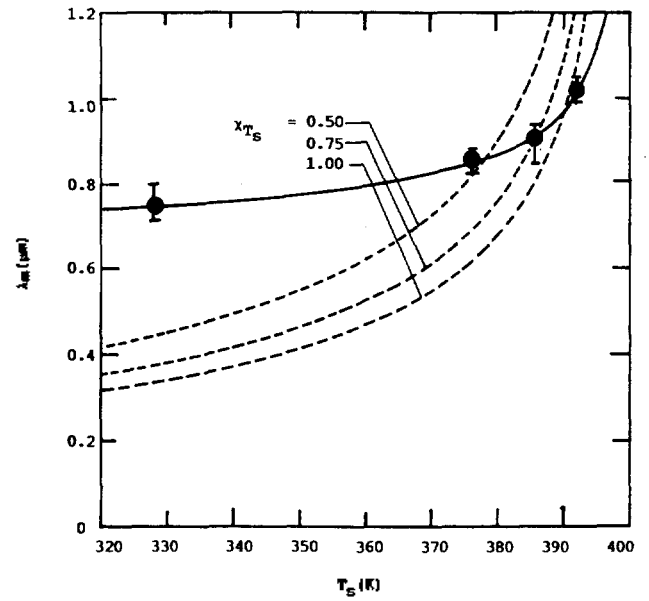

Figure 5. The fastest growing wave length, λ_m, plotted as a function of quench temperature. The black closed circles of the picture represent the experimental values of Aarsten and Smolders.[21] Three dashed lines represent the results of the original theory of Balsara and Nauman for three values of χ_{T_s}. The solid line represents the calculated curve of our present theory for the χ_{T_s} value of 0.63.

concentration of solutions, temperature, and so on, the values of q of two sample strands differ from each other. It is self-evident that the farther the distance between strands is, the smaller the probability of contact between strands is. In figures 3 and 4, the value of $h_p(d)$ is greater than that of $g_p(d)$ because the double contact probability is greater than the single contact one due to the character resulting from the relatively long length of a strand.

In Figure 5, the fastest growing wave length, λ_m, is plotted

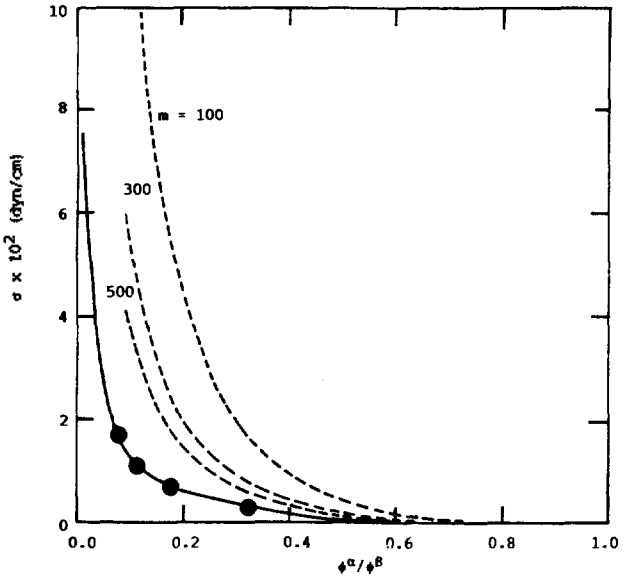

Figure 6. Interfacial tension between demixed polymer solutions as a function of the ratio of the polymer concentration in the dilute phase to that in the concentrated phase. The black closed circles represented the experimental data of Nose and Tan[22] for the polystyrene-methylcyclohexane system ($m=300$). Three dashed lines represent the result of the original Balsara and Nauman's theory for three values of m. The solid line represents the result of our present theory for the m value of 300.

as a function of quench temperature. The black closed circles of the picture represent the experimental values of Aarsten and Smolders.[21] Three dashed lines represent the results of the original theory of Balsara and Nauman for three values of χ_{T_s}. The solid line represents the calculated curve of our present theory for the χ_{T_s} value of 0.63. In other words, three dashed lines represent the results of Eq. (37'), and the solid line the result of Eq. (37). From the comparison of our present theory with the original Balsara and Nauman's, it is exposed that the discrepancy between the results of the Balsara and Nauman's theory and the experimental data essentially results from the fact that the Balsara and Nauman's theory did not include the effects of interaction between polymer strands in calculating the entropy of polymer-solvent systems. The experimental sample related with Figure 5 is a 15% (by weight) solution of poly(2,6-dimethyl-1,4-phenyleneether)[PPE] and caprolactam. The values of parameters used in calculation are such as $R_G=0.02$ μm, $\phi=0.15$, $\chi_{T_s}=0.63$, and $q=0.47$ $m^{1/2}a$. From Figure 5, we see that the effect of interaction between strands is larger at the higher quench depth than at the lower quench depth. It is judged that such an aspect results from the fact that for the higher quench depth the time interval about rearrangement of polymer networks so the probability of interaction between strands is greater.

In Figure 6, there is shown interfacial tension between demixed polymer solutions as a function of the ratio of the polymer concentration in the dilute phase to that in the concentrated phase. The black closed circles represented the experimental data of Nose and Tan[22] for the polystyrene-methylcyclohexane system ($m=300$). Three dashed lines repre-

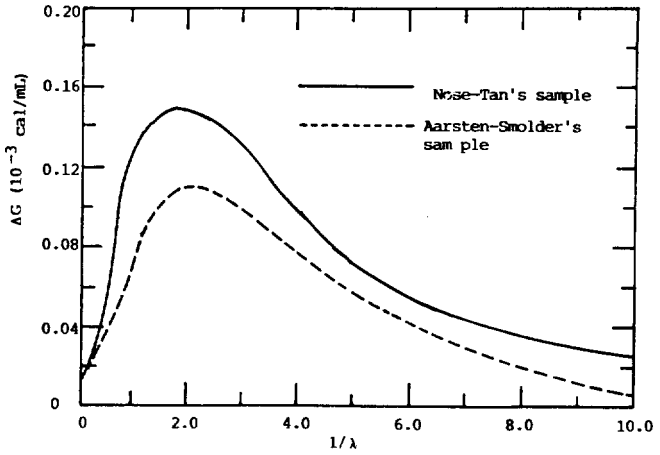

Figure 7. The free energy curves obtained from Eqs. (30), (31), and (34). The solid line represents the result of the Nose-Tan's sample, and the dashed one represents that of the Aarsten-Smolders's sample.

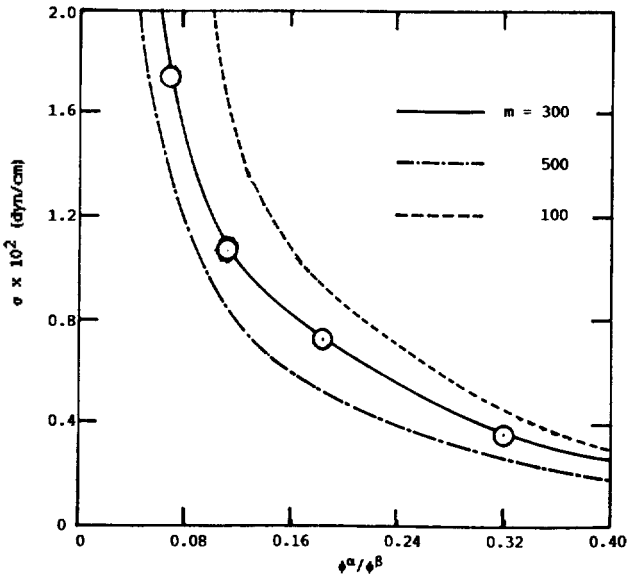

Figure 8. The picture having enlarged Figure 6. As shown previously, the open circles are the experimental data points. Three calculated curves of our present theory are offered according to three given values of m.

sent the result of the original Balsara and Nauman's theory for three values of m. The solid line represents the result of our present theory for the m value of 300. In other words, three dashed lines represent the results of Eq. (44'), and the solid line the result of Eq. (44). Comparing our present theory with the original Balsara and Nauman's, we see that the discrepancy between the results of the Balsara and Nauman's theory and experimental data is essentially caused by the fact that the Balsara and Nauman's theory did not include the effects of interaction between polymer strands in calculating the entropy of polymer-solvent systems. The experimental sample used in Figure 6 is demixed polystyrene (molecular weight=37,000)-methylcyclohexane. Such experiments were carried out by Nose and Tan,[22] and they measured the interfacial tension as a function of temperature in addition to the coexistence curve for the system. Thus there can be deduced the dependence of the interfacial tension on the composition of the two phases at equilibrium. The fact that the ratio of the densities of polystyrene to methylcyclohexane in solution has the value of 1.4 is used in converting polymer weight fractions to volume fractions. the values of parameters or constants used in calculation are such as $R_G=0.27\ m^{1/2}$ nm, $\bar{v}_s=128$ cm³/mol, $m=300$, and $T=300$ °K. From Figure 6, it is known that the effect of interaction between strands is larger at the lower concentration ratio than at the higher concentration ratio, ϕ^α/ϕ^β. It is judged that such an aspect results from the fact that since for the lower relative concentration ratio, the structure of polymer networks between two liquid phases nearly resembles each other, so the total interaction between strands over two liquid phases is more largely increased.

In Figure 7, the free energy curves obtained from Eqs. (30), (31), and (34) are plotted over the reciprocal strain, $1/\lambda$. The solid line represents the result of the Nose-Tan's sample, and the dashed one represents that of the Aarsten-Smolders's sample. Since for the Nose-Tan's sample the distance between strands is smaller than for the Aarsten-smolders's sample, it is self-evident that the values of the free energy curve of the Nose-Tan's is larger than those of Aarsten-Smolders's. The values of parameters used in calculation are the same as those of Figures 5 and 6.

In Figure 8, the picture having enlarged Figure 6 is shown. As shown previously, the open circles are the experimental data points. Three calculated curves of our present theory are offered according to three given values of m (*i.e.*, 100, 300, and 500).

Conclusion

The original Balsara and Nauman's theory, a kind of phantom network theory, for polymer-solvent systems has been expanded by adding the term of the topological interaction between strands, so our extended theory explains very well the characteristics of spinodal decomposition and interfacial tension of polymer-solvent systems. The polymer-solvent systems considered here are assumed to have the structure of the THL network composed of polymer solutes and solvents. It is judged that the discrepancy between the experimental data and the original Balsara and Nauman's theory results from the fact that their original theory did not include the results of interaction between strands.

It is exposed that the results of the expended theory show good agreement with the given experimental data.

Finally, it is judged that the assumption of the THL structure for the given polymer-solvent systems is very reasonable, based upon the fact that the extened theory explains very well the given experimental data.

Acknowledgment. The Present Studies were Supported (in part) by the Basic Science Research Institute Program, Ministry of Education, 1994. Project No. BSRI-94-3414.

References

1. Flory, P. J.; Rehner, J. J. *J. Chem. Phys.* **1943**, *11*, 521.

2. Edwards, S. F.; Freed, K. F. *J. Phys. C.* **1970**, *3*, 760.
3. Graessley, W. W. *Macromolecules* **1975**, *8*, 865.
4. Ronca, G.; Allegera, G. *J. Chem. Phys.* **1975**, *63*, 4990.
5. Flory, P. J. *Proc. R. Soc. London Ser. A.* **1976**, *351*, 351.
6. Ziabicki, A.; Walasek, J. *Macromolecules* **1978**, *11*, 471.
7. Langley, N. R. *Macromolecules* **1968**, *1*, 348.
8. Deam, R. T.; Edwards, S. F. *Philos. Trans. R. Soc. London Ser. A* **1976**, *66*, 3363.
9. Graessley, W. W.; Pearson, D. S. *J. Chem. Phys.* **1977**, *66*, 3363.
10. Iwata, K.; Kurata, M. *J. Chem. Phys.* **1969**, *50*, 4008.
11. Iwata, K. *J. Chem. Phys.* **1980**, *73*, 562. **1981**, *74*, 2039. **1983**, *78*, 2778. **1985**, *83*, 1969.
12. Iwata, K. *J. Chem. Phys.* **1982**, *76*, 6363. **1982**, *ibid* 6375.
13. Son, J. M.; Pak, H. *Bull. Korean Chem. Soc.* **1989**, *10*, 84.
14. Son, J. M.; Pak, H. *Proc. Coll. Natur. Sci., SNU* **1988**, *13*, 47.
15. Son, J. M.; *Ph. D. Thesis, SNU, Seoul, Korea, 1989.*
16. *Flory, P. J. J. Chem. Phys.* **1942**, *10*, 51.
17. Balsara, N. P.; Nauman, E. B. *J. Polymer Sci.* **1988**, *26*, 1077.
18. Cahn, J. W.; Hilliard, J. E. *J. Chem. Phys.* **1958**, *28*, 258.
19. Cahn, J. M. *Trans. Metal. Soc.* **1968**, *242*, 166.
20. van Aarsten, J. J. *Europ. Polymer J.* **1970**, *6*, 919.
21. van Aarsten, J. J.; Smolders, C. A. *Europ. Polymer J.* **1970**, *6*, 1105.
22. Nose, T.; Tan, T. V. *J. Polym. Sci. Polym. Lett. Ed.* **1976**, *14*, 705.

Mechanistic Significances of the Reactivity-Selectivity Principle

Ikchoon Lee, Bon-Su Lee*, Han Joong Koh, and Byung Doo Chang†

Department of Chemistry, Inha University, Inchon 402-751, Korea
†Department of Chemistry, Inchon University, Inchon 402-749, Korea
Received December 29, 1994

The relationship between the signs of $\rho_{i(0)}$, $\rho_{j(0)}$ and ρ_{ij} and validity of the reactivity-selectivity principle (RSP) has been derived: RSP is valid when $W=\rho_{i(0)}\cdot\rho_{j(0)}/\rho_{ij}$ is negative. The analysis of 100 reaction series indicated that for normal S_N2 reactions involving variations of substituents in the nucleophile (X) and in the substrate (Y) RSP is valid only for a dissociative type for which $\rho_{Y(0)}$ is negative, whereas for the acyl transfer reactions with rate-limiting breakdown of the tetrahedral intermediate RSP is valid in general for all substituent changes, X, Y and/or Z (substituent on the leaving group). The trends in the validity of RSP for certain types of reaction can be useful in supplementing the mechanistic criteria based on the signs of $\rho_{i(0)}$, $\rho_{j(0)}$ and ρ_{ij}.

Introduction

Increasing reactivity of a reagent is often accompanied by decreasing selectivity. This so-called Reactivity-Selectivity Principle (RSP)[1] has attracted considerable interests of experimental organic chemists. However, usefulness of RSP as a general rule has been questioned, because there are so many experimental examples of invalid cases.[2] Recently, Exner[3] has shown in his work involving statistical examination of RSP with 100 reaction series that RSP is valid only in half (50%) of the cases studied. He concluded, however, that although RSP is not evidently a general rule "investigations of selectivity and its relation to reactivity should be continued and used possibly to characterize a certain type of reaction or a certain mechanism".

For the past several years we have been developing the cross-interaction constants, ρ_{ij} in eq. 1,[4] as a mechanistic tool for organic reactions in solution.

$$\log(k_{ij}/k_{00})=\rho_{i(0)}\sigma_i+\rho_{j(0)}\sigma_j+\rho_{ij}\sigma_i\sigma_j \quad (1)$$

For a typical S_N2 TS, Scheme 1, i, j=X, Y or Z where *X, Y and Z represent the nucleophile, substrate and leaving group,*

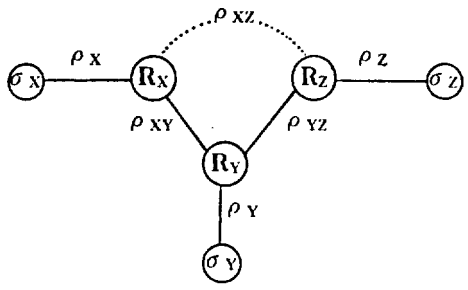

Scheme 1.

respectively. $\rho_{i(o)}$ (or $\rho_{j(o)}$) denotes the Hammett ρ value for variation of σ_i (or σ_j) with $\sigma_j=0$ (or $\sigma_i=0$).

In this work, we examine the relationship between the signs of $\rho_{i(0)}$, $\rho_{j(0)}$ and ρ_{ij} and the validity of RSP, which can be used to characterize a certain type of reaction or mechanism, as Exner has suggested in his paper.

Derivation of the Relationship

Let us consider a simple reaction system consisting of